Atmos. Meas. Tech. Discuss., 3, 3987–4007, 2010
www.atmos-meas-tech-discuss.net/3/3987/2010/
doi:10.5194/amtd-3-3987-2010

Atmospheric Measurement Techniques Discussions

Remote sensing of water vapour profiles in the framework of the Total Carbon Column Observing Network (TCCON)

M. Schneider[1,*], **E. Sepúlveda**[2,3], **O. García**[3], **F. Hase**[1], **and T. Blumenstock**[1]

[1]Karlsruhe Institute of Technology (KIT), IMK-ASF, Karlsruhe, Germany
[2]University of La Laguna, La Laguna, Spain
[3]Agencia Estatal de Meteorología (AEMET), CIAI, Santa Cruz de Tenerife, Spain
[*]now at: Agencia Estatal de Meteorología (AEMET), CIAI, Santa Cruz de Tenerife, Spain

Received: 15 July 2010 – Accepted: 27 August 2010 – Published: 31 August 2010

Correspondence to: M. Schneider (matthias.schneider@kit.edu)

Published by Copernicus Publications on behalf of the European Geosciences Union.

Abstract

We show that the near infrared solar absorption spectra recorded in the framework of the Total Carbon Column Observing Network (TCCON) can be used to derive the vertical distribution of tropospheric water vapour. Using spectral H_2O signatures in the 4500–4700 cm^{-1} region one can well distinguish lower from middle/upper tropospheric water vapour concentrations. The vertical resolution is about 3 and 6 km, for the lower and middle/upper troposphere, respectively. We document the quality of the remotely-sensed profiles by comparisons with coincident in-situ Vaisala RS92 radiosonde measurements. The agreement of both techniques is very satisfactory. Due to the long-term strategy of the network and the high measurement frequency, the TCCON water vapour profile data offer novel opportunities for estimating the water vapour variability at different time scales and altitudes.

1 Introduction

During the last years large investments have been undertaken to set up the Total Carbon Column Observing Network (TCCON, www.tccon.caltech.edu) as a quasi-automated monitoring network. A TCCON experiment consists of a high precision solar tracker and a high quality ground-based Fourier Transform Spectrometer (FTS). A big shipping container is typically used as housing of the equipment whose overall material costs are about 500 kEUR. In the meanwhile there are about 15 globally-distributed FTS experiments operating in the framework of the TCCON. The experiments record direct solar spectra in the near-infrared spectral region (4000–9000 cm^{-1}). In this spectral region there are distinct rotational-vibrational bands of the atmospheric trace gases CO_2, CH_4, N_2O, HF, CO, H_2O, and HDO. The TCCON will focus on the measurement of accurate and precise column-averaged abundances of the greenhouse gases CO_2, CH_4, and N_2O (e.g., Yang et al., 2002; Washenfelder et al., 2006; Wunch et al., 2010). Concerning CO_2 a precision of 0.2%, i.e., about 0.8 ppm is targeted. This high preci-

AMTD
3, 3987–4007, 2010

sion is essential for using the column-averaged data in carbon cycle research (Olsen and Randerson, 2004). However, this is a very challenging objective and consequently there are strong quality requirements on the TCCON partners: at almost all sites very stable FTS are applied (Bruker IFS 125HR), the performance of the instruments (e.g., instrumental line shape, Hase et al., 1999) has to be reported on a regular basis, etc.

These challenging TCCON objectives assure that the solar absorption spectra will be measured for many years, at several globally distributed sites, and with very high quality. It offers interesting opportunities for ground-based remote sensing and long-term atmospheric studies. Water vapour is a very important atmospheric trace gas and understanding all the processes that influence the vertical distribution of water vapour are of interest for weather as well as climate prediction. For instance, it is the middle/upper troposphere and the lower stratosphere where water vapour acts most efficiently as greenhouse gas (Spencer and Braswell, 1997). Atmospheric water vapour is a key player concerning climate variability and climate patterns (Randall et al., 2007). Producing water vapour profiles from TCCON spectra would be very interesting for climate studies.

Ground-based solar absorption spectra measured in the middle infrared in the framework of the Network for the Detection of Atmospheric Composition Change (NDACC, Kurylo and Zander, 2000, www.acd.ucar.edu/irwg) allow the remote sensing of tropospheric water vapour profiles (Schneider et al., 2006, 2010a; Schneider and Hase, 2009). More recently, Schneider et al. (2010c) show that the water vapour profiles retrieved from near infrared signatures (4500–4700 cm^{-1}) are also of very good quality. However, the so far applied spectra have been highly-resolved (spectral resolution of 0.0025–0.0075 cm^{-1}), whereas the resolution of the TCCON spectra is limited to 0.02 cm^{-1}. In this paper we show that this resolution is still sufficient to derive tropospheric water vapour profiles and that it enables a high measurement frequency. In Sect. 2 we briefly describe the measurement principle of TCCON and the generalities of evaluating high resolution solar absorption spectra and the set up of the TCCON water vapour profile retrieval. Section 3 characterises and validates the profiles and

AMTD
3, 3987–4007, 2010

Sect. 4 demonstrates the unique measurement frequency of the TCCON water vapour profiles. The paper ends with a summary (Sect. 5).

2 A TCCON experiment and the principles of ground-based infrared remote sensing

Figure 1 shows the two main components of a TCCON experiment: a precise solar tracker (left photograph) that captures the direct solar light beam and a high resolution FTS (right photograph). For TCCON the FTS measures in the 4000–9000 cm^{-1} region with a resolution of 0.02 cm^{-1} (i.e., maximum optical path difference, OPD, of 45 cm). This corresponds to a resolution power $\lambda/\Delta\lambda$ at 5000 cm^{-1} of approx. 2.5×10^5. Recording of one spectrum requires between 30 s and a few minutes, depending on the quality needed: one scan can be performed in 30 s, but often several scans are co-added in order to increase the signal to noise ratio. Together with the AC-signal, the DC-signal of the interferogram is recorded. This allows correcting for inhomogeneous sky conditions, like cirrus cloud cover (Keppel-Aleks et al., 2007). No observations can be performed for a sky covered with optically thick clouds.

The basic equation for analysing near infrared solar absorption spectra is Lambert Beer's law:

$$I(\lambda) = I_{\text{sun}}(\lambda)\exp\left(-\int_{\text{TOA}}^{\text{Obs.}} \sigma_x(\lambda, s(T,p))x(s)ds\right) \quad (1)$$

Here $I(\lambda)$ is the measured intensity at wavelength λ, I_{sun} the solar intensity, $\sigma_x(\lambda,s)$ is the absorption cross section and $x(s)$ the concentration of an absorber x at location s. The integration is performed along the path of the direct sunlight (from the top of the atmosphere (TOA) to the observer). The cross section σ_x depends on temperature and pressure. The measurement $I(\lambda)$ is simulated by a precise line-by-line radiative transfer model, whereby the HITRAN parameters are applied (Rothman et al., 2009). The radiative transfer model includes a ray tracing module (e.g., Hase and Höpfner,

AMTD
3, 3987–4007, 2010

1999) in order to determine how the solar light passes through the different atmospheric layers.

By means of the discretisation we can describe the vertical distribution of the absorber in form of a vector $\boldsymbol{x}(z)$ (concentration of absorber x at level z). If we also describe the simulated spectrum, $I(\lambda)$, in form of a vector $\boldsymbol{y}$ containing the radiances in the different spectral bins, we can define a forward relation, F, that connects the the solar absorption spectrum ($\boldsymbol{y}$) to the vertical distribution of the absorber ($\boldsymbol{x}$), to parameters describing the atmospheric state ($\boldsymbol{p}_{\text{atmos}}$), and to parameters describing the measurement system ($\boldsymbol{p}_{\text{exp}}$) :

$$\boldsymbol{y} = \boldsymbol{F}(\boldsymbol{x}, \boldsymbol{p}_{\text{atmos}}, \boldsymbol{p}_{\text{exp}}) \tag{2}$$

Here $\boldsymbol{F}$ is a vector valued function which simulates the atmospheric radiative transfer and the characteristics of the measurement system (spectral resolution, instrumental line shape, etc.).

The derivatives $\partial y / \partial x$ determine the changes in the spectral fluxes $\boldsymbol{y}$ for changes in the vertical distribution of the absorber $\boldsymbol{x}$. These derivatives are sampled in a Jacobian matrix $\mathbf{K}$:

$$\partial \boldsymbol{y} = \mathbf{K} \partial \boldsymbol{x} \tag{3}$$

Inverting $\mathbf{K}$ of Eq. 3 would allow an iterative calculation of the sought variables $\boldsymbol{x}$, but deriving the vertical distribution of an atmospheric absorber is an under determined problem, i.e. the columns of $\mathbf{K}$ are not linearly independent and there are many solutions that are in acceptable agreement with the measurement. We cannot derive a unique solution but we can estimate the most probable solution for the given measurement. This optimal estimation (OE) approach combines the measurement information with a priori knowledge and provides the most probable solution by minimising the following cost function:

$$[\boldsymbol{y} - \boldsymbol{F}(\boldsymbol{x})]^T \mathbf{S}_\varepsilon{}^{-1} [\boldsymbol{y} - \boldsymbol{F}(\boldsymbol{x})] + [\boldsymbol{x} - \boldsymbol{x}_a]^T \mathbf{S}_\mathbf{a}{}^{-1} [\boldsymbol{x} - \boldsymbol{x}_a] \tag{4}$$

AMTD
3, 3987–4007, 2010

Where $\mathbf{S}_\epsilon$ is the noise covariance, $\boldsymbol{x}_a$ and $\mathbf{S}_a$ are the a-priori known mean distribution and the covariance of the distribution of the absorber, respectively. For more details about OE approaches please refer to the textbook of C. D. Rodgers (Rodgers, 2000).

The optimal estimation of atmospheric water vapour amounts from ground-based FTIR spectra is far from being a typical atmospheric inversion problem and, due to its large vertical gradient and variability, standard retrieval methods are not appropriate. Only very recently the ground-based infrared remote sensing of water vapour profiles has become feasible. Among others, it requires the inversion to be performed on a logarithmic scale (Schneider et al., 2006) and the application of a speed dependent Voigt line shape model (Schneider et al., 2010d, and references therein). A review of water vapour profile analysis methods is given in Schneider and Hase (2009). For the near infrared retrieval we fit the spectral microwindows as depicted in Fig. 2 and use the retrieval code PROFFIT (Hase et al., 2004).

3 Characterisation and validation of the profiles

Atmospheric profiles remotely-sensed by ground-based instruments offer – compared to in-situ measurements – a limited vertical resolution. The vertical structures that are detectable are documented by the averaging kernels. Figure 3 depicts a typical set of averaging kernels for water vapour profile retrievals when applying the near infrared microwindows of Fig. 2. In order to assess the effect of spectral resolution on the vertical resolution of the remote sensing system we measured spectra with different spectral resolution (0.004 cm^{-1}, 0.02 cm^{-1}, 0.1 cm^{-1}, and 0.5 cm^{-1}) during 20 min on a stable day and for typical conditions (typical water vapour content, solar elevation angle, aerosol loading, etc.). The averaging kernels for 3, 5, and 8 km (representative for the lower, middle and upper troposphere) are highlighted by red, blue and green colors, respectively. The sum along the rows of the averaging kernel matrix documents the sensitivity of the remote sensing system. It is depicted as thick black line. For high spectral resolution (typical for NDACC measurements) we can detect 2 km thick layers

AMTD
3, 3987–4007, 2010

in the lower troposphere, 4 km layers in the middle troposphere, and 7 km layers in the upper troposphere. Then the sensitivity is almost optimal (close to unity) throughout the whole troposphere, which means that the FTIR system is well able to detect the atmospheric variability between the surface and an altitude of about 12.4 km, where still 75% of the real atmospheric variability can be detected by the remote sensing system. Measuring a high resolution NDACC spectra takes about 8 min. If we reduce the spectral resolution to 0.02 cm^{-1} – which is the resolution of TCCON spectra – the middle and upper tropospheric averaging kernels become broader, but on the other hand the measurement time reduces to 2 min. With TCCON spectra lower tropospheric water vapour concentrations can still be well distinguished from middle/upper tropospheric concentrations and we can measure a profile each 2 min. However, then the > 75% sensitivity range is limited to altitudes below 10.7 km. For a spectral resolution of 0.1 cm^{-1} the measurement time but also the sensitivity range get further reduced, but we still can distinguish water vapour variations that occur above 6 km altitude from variation close to the surface. If we reduce the spectral resolution to 0.5 cm^{-1} a measurement takes just a few seconds, but then the system is not well able to separate water vapour variations that occur at different altitudes and it is only satisfactorily sensitive below an altitude of 6.3 km. Figure 4 shows how the degree of freedom of the measurement (dof) depends on the spectral resolution. The dof value is a measure of the amount of information that is introduced by the measurement. It is about 2.5 for high resolution spectra, 2.3 for TCCON spectra, and about 2 for 0.1 cm^{-1} spectral resolution, which seems to be the limit for identifying two independent atmospheric layers. For a poorer spectral resolution the dof value is below 2 and the profiling capability of the system is limited. The TCCON resolution is a good compromise enabling both, good vertical resolution and high measurement frequency.

The vertical resolution that is achieved with TCCON spectra is only slightly reduced if compared to the profiles retrieved from the NDACC high resolution spectra. The spectra contain information about the vertical distribution of the absorber mainly due to the pressure broadening effect (lines are the broader the higher the pressure at the

AMTD
3, 3987–4007, 2010

absorbers location). The broadening coefficients are typically 0.04–0.08 $cm^{-1}atm^{-1}$. At the tropopause the pressure is still high (e.g., 0.2 atm at 12 km). For a retrieval of tropospheric profiles a spectral resolution of 0.02 cm^{-1} (or even 0.1 cm^{-1}) is obviously sufficient, whereas a ground-based infrared remote sensing of stratospheric profiles, e.g., for investigating the ozone layer, is only feasible with the high resolution spectra of the NDACC.

The near infrared spectra allow a retrieval of H_2O profiles but not of HDO profiles. Above 3000 cm^{-1} the signatures of the latter are rather weak. Profiles of HDO/H_2O are very interesting for water cycle research (e.g., Worden et al., 2007; Frankenberg et al., 2009; Schneider et al., 2010b). HDO/H_2O profiles can be remote sensed from ground with the NDACC mid-infrared spectra but not with TCCON's near infrared spectra.

At Tenerife Island radiosondes (Vaisala RS92) are launched twice per day (23:15 UT and 11:15 UT). The launch site is just about 15 km southeast of the Observatory on the coastline. The radiosonde measurements offer a good opportunity for validating the FTIR profiles (e.g. Schneider et al., 2010a). Figure 5 documents the agreement between radiosonde and FTIR profiles measured in coincidence between April and June 2010. The profiles are shown as relative difference to climatological values, which allows a clear presentation despite the the large vertical gradient (lower and upper tropospheric water vapour concentrations differ typically by two orders of magnitude). The small black squares show the RS92 profiles after correction of temperature effects and radiation bias (Miloshevich et al., 2009). These in-situ profiles offer a very high vertical resolution. To the contrary, the remote sensing technique only allows resolving rather rough vertical structures (see averaging kernels of Fig. 3). For an adequate comparison we have to degrade the RS92 profiles to the vertical resolution of the FTIR profiles. Therefore, we convolve the vertically highly-resolved RS92 profiles (x_{RS92}) with the FTIR averaging kernels $\hat{\mathbf{A}}$:

$$\hat{x}_{RS92} = \hat{\mathbf{A}}(x_{RS92} - x_a) + x_a \quad (5)$$

The result is a smoothed RS92 profile ($\hat{x}_{RS92}$) with the same vertical resolution as

AMTD
3, 3987–4007, 2010

the FTIR profile (x_a in Eq. (5) stands for the a priori climatological mean profile). The black stars in Fig. 5 depict the $\hat{x}_{RS92}$ profiles. Their comparison to the vertically highly-resolved profiles (black squares) gives a good impression about the vertical H_2O structures that can theoretically be measured by a TCCON experiment. A good example is the unusual profile shape on day 100426: the FTIR system is able to detect the very low concentrations in the lower troposphere (below 200 ppm between 3 and 4.5 km, i.e. only 10% of the typical concentration) and the extraordinary high middle/upper tropospheric water vapour amounts (e.g., above 2000 ppm at 6.5 km, i.e. almost 5 times more than the typical concentration), but it cannot resolve the fine structures in the middle/upper troposphere (high concentrations at 6, 8 and 10 km alternate with low concentrations at 7, 9 and 11 km). The red circles represent the profiles as retrieved from the TCCON spectra. For the coincidences shown in Fig. 5 FTIR and smoothed RS92 profiles agree very well, which confirms more extensive comparison studies (e.g. Schneider et al., 2010a,c).

4 Time scale analysis

Spectra with a resolution of $0.02\,cm^{-1}$ are measured in less than 2 min. TCCON can provide a uniquely dense set of solar absorption spectra, which can be used to detect variation in the tropospheric water vapour distribution on different time scales ranging from a few minutes up to several days. Figure 6 shows the diurnal evolution of lower and upper tropospheric H_2O concentration as obtained from TCCON measurements at Izaña. The values are given in $\ln\hat{x} - \ln x_a \approx 2 \times \frac{\hat{x}-x_a}{\hat{x}+x_a}$, whereby $\hat{x}$ represents the retrieved water vapour concentrations and x_a the a priori climatological mean concentrations. On this day we measured about 90 near infrared spectra between 12:30 UT and 16:30 UT. The lower tropospheric concentrations are significantly increased between 13:45 and 14:30 UT. This is due to local effects: the land mass heats during the morning hours, which gives rise to surface near turbulence after local noon. In the upper troposphere the diurnal evolution is rather smooth. There the water vapour concentrations are rather

AMTD
3, 3987–4007, 2010

constant during the whole day.

We find that this is a typical situation. Figure 7 plots profiles of the tropospheric water vapour variability on different time scales as obtained from TCCON measurements. The study bases on measurements taken at Izaña on 10 days between April and June 2010 with 50–100 profile measurements on each of these days. We define the variability as the 1σ standard deviation of the logarithm of the water vapour concentration. This is equivalent to the variability relative to a mean value of the considered time period. We do not claim that this is a comprehensive study, since therefore we should analyse more data, instead our intention is to reveal the potential of a uniquely dense data set of tropospheric water vapour profiles. We observe that most variability occurs on time scales that are larger than 1 day. However, even on short-time scales lower tropospheric variabilities cannot be neglected. Within three hours only, lower tropospheric water vapour already varies by 15%, which is clearly larger than the estimated measurement uncertainty (dotted black line). The significant variability on short time scales converts the inter-comparison of lower tropospheric water vapour measurement techniques into a difficult task. It is strongly recommendable that the different techniques measure at exactly the same time. The variability on short time-scales also points to small-scale structures in the horizontal water vapour fields of the lower troposphere. When comparing different techniques we must assure that the different experiments detect the same airmasses, already slightly different airmasses can introduce significant uncertainties in the inter-comparison study. The situation is a bit less critical in the middle/upper troposphere, where the variability on time scales smaller than 3 h is reduced to 10%. It seems that the middle/upper troposphere is more stable and changes are smoother in time as well as in space.

5 Conclusions

TCCON is a rather new and expensive network of high quality ground-based FTS systems. Its long-term strategy is very attractive for many fields of atmospheric research,

AMTD
3, 3987–4007, 2010

in particular for climate change research. Atmospheric water vapour is a key player for the Earth's climate. We show that TCCON measurements can be used to produce a dense long-term H_2O profile data set with a satisfactory quality. The vertical resolution is modest but still allows separating lower from middle/upper tropospheric water vapour amounts. The density of the profile data would be unique and would offer novel opportunities in different research fields:

- It would allow an estimation of tropospheric water vapour variabilities on different time scales and for different altitudes. This is important for assessing the validity and limits of water vapour profile inter-comparison studies.
- It would help when assimilating water vapour observations into atmospheric models. The observations are often sparse in time and space and for a proper assimilation it is important to know about the variability time scales and the spatial homogeneity of water vapour. TCCON data could constrain some of these unknowns.
- It would allow an unprecedented study of small scale processes and a statistical validation of tropospheric high resolution models. Thereby, it could help to investigate the processes that determine upper tropospheric humidity (convective processes, evaporation from cloud droplets, lateral mixing, etc.). The currently limited understanding of upper tropospheric humidity is a main uncertainty source of climate prediction models.

Acknowledgements. M. Schneider has been supported by the Deutsche Forschungsgemeinschaft via the project RISOTO (Geschäftszeichen SCHN 1126/1-1 and 1-2) and since May 2010 he enjoys a Ramón y Cajal grant from the Spanish Ministry of Science and Innovation. E. Sepúlveda receives a predoctoral fellowship from the Spanish Ministry of Education. The establishment of TCCON was generously supported by grants from NASA's terrestrial carbon cycle program and from the OCO project office. We are grateful to the Goddard Space Flight Center for providing the temperature and pressure profiles of the National Centers for Environmental Prediction via the automailer system.

AMTD
3, 3987–4007, 2010

References

Frankenberg, C., Yoshimura, K., Warneke, T., Aben, I., Butz, A., Deutscher, N., Griffith, D., Hase, F., Notholt, J., Schneider, M., Schrejver, H., and Röckmann, T.: Dynamic processes governing lower-tropospheric HDO/H_2O ratios as observed from space and ground, Science, doi:10.1126/science.1173791, 325, 1374–1377, 2009. 3994

Hase, F., Blumenstock, T., and Paton-Walsh, C.: Analysis of the instrumental line shape of high-resolution Fourier transform IR spectrometers with gas cell measurements and new retrieval software, Appl. Optics, 38, 3417–3422, 1999. 3989

Hase, F. and Höpfner, M.: Atmospheric raypath modelling for radiative transfer algorithms, Appl. Optics, 38, 3129-3133, 1999. 3990

Hase, F., Hannigan, J. W., Coffey, M. T., Goldman, A., Höpfner, M., Jones, N. B., Rinsland, C. P., and Wood, S. W.: Intercomparison of retrieval codes used for the analysis of high-resolution, ground-based FTIR measurements, J. Quant. Spectrosc. Ra., 87, 25–52, 2004. 3992

Keppel-Aleks, G., Toon, G. C., Wennberg, P. O., and Deutscher, N. M.: Reducing the impact of source brightness fluctuations on spectra obtained by Fourier-transform spectrometry, Appl. Optics, 46, 4774–4779, 2007. 3990

Kurylo, M. J. and Zander, R.: The NDSC – Its status after 10 years of operation, Proceedings of XIX Quadrennial Ozone Symposium, Hokkaido University, Sapporo, Japan, 167–168, 2000. 3989

Miloshevich, L. M., Vömel, H., Whiteman, D. W., and Leblanc, T.: Accuracy assessment and correction of Vaisala RS92 radiosonde water vapor measurements, J. Geophys. Res., 114, D11305, doi:10.1029/2008JD011565, 2009. 3994, 4005

Olsen, S. C. and Randerson, J. T.: Differences between surface and column atmospheric CO_2 and implications for carbon cycle research, J. Geophys. Res., 109, D02301, doi:10.1029/2003JD003968, 2004. 3989

Randall, D. A., Wood, R. A., Bony, S., Colman, R., Fichefet, T., Fyfe, J., Kattsov, V., Pitman, A., Shukla, J., Srinivasan, J., Stouffer, R. J., Sumi, A., and Taylor, K. E.: Climate Models and Their Evaluation, in: Climate Change 2007: The Physical Science Basis, Contribution of Working Group I to the Fourth Assessment Report of the Intergovernmental Panel on Climate Change, edited by: Solomon, S., Qin, D., Manning, M.,Chen, Z., Marquis, M., Averyt, K. B., Tignor, M., and Miller, H. L., Cambridge University Press, Cambridge, UK and New York, NY, USA, 2007. 3989

AMTD
3, 3987–4007, 2010

Rodgers, C. D.: Inverse Methods for Atmospheric Sounding: Theory and Praxis, World Scientific Publishing Co., Singapore, ISBN 981-02-2740-X, 2000. 3992

Rothman, L. S., Gordon, I. E., Barbe, A., Chris Benner, D., Bernath, P. F., Birk, M., Boudon, V., Brown, L. R., Campargue, A., Champion, J.-P., Chance, K., Coudert, L. H., Dana, V., Devi, V. M., Fally, S., Flaud, J.-M., Gamache, R. R., Goldman, A., Jacquemart, D., Kleiner, I., Lacome, N., Lafferty, W. J., Mandin, J.-Y., Massie, S. T., Mikhailenko, S. N., Miller, C. E., Moazzen-Ahmadi, N., Naumenko, O. V., Nikitin, A. V., Orphal, J., Perevalov, V. I., Perrin, A., Predoi-Cross, A., Rinsland, C. P., Rotger, M., Simecková, M., Smith, M. A. H., Sung, K., Tashkun, S. A., Tennyson, J., Toth, R. A., Vandaele, A. C., and Vander-Auwera, J.: The HITRAN 2008 molecular spectroscopic database, J. Quant. Spectrosc. Ra., 110, 533–572, doi:10.1016/j.jqsrt.2009.02.013, 2009. 3990

Schneider, M., Hase, F., and Blumenstock, T.: Water vapour profiles by ground-based FTIR spectroscopy: study for an optimised retrieval and its validation, Atmos. Chem. Phys., 6, 811–830, doi:10.5194/acp-6-811-2006, 2006. 3989, 3992

Schneider, M. and Hase, F.: Ground-based FTIR water vapour profile analyses, Atmos. Meas. Tech., 2, 609–619, doi:10.5194/amt-2-609-2009, 2009. 3989, 3992

Schneider, M., Romero, P. M., Hase, F., Blumenstock, T., Cuevas, E., and Ramos, R.: Continuous quality assessment of atmospheric water vapour measurement techniques: FTIR, Cimel, MFRSR, GPS, and Vaisala RS92, Atmos. Meas. Tech., 3, 323–338, doi:10.5194/amt-3-323-2010, 2010a. 3989, 3994, 3995

Schneider, M., Yoshimura, K., Hase, F., and Blumenstock, T.: The ground-based FTIR network's potential for investigating the atmospheric water cycle, Atmos. Chem. Phys., 10, 3427–3442, doi:10.5194/acp-10-3427-2010, 2010b. 3994

Schneider, M., Toon, G. C., Blavier, J.-F., Hase, F., and Leblanc, T.: H_2O and δD profiles remotely-sensed from ground in different spectral infrared regions, Atmos. Meas. Tech. Discuss., 3, 3105–3132, doi:10.5194/amtd-3-3105-2010, 2010c. 3989, 3995

Schneider, M., Hase, F., Blavier, J.-F., Toon, G. C., and Leblanc, T.: An empirical study on the importance of a speed-dependent Voigt line-shape model in different water vapor bands, submitted, J. Quant. Spectrosc. Ra., 2010d. 3992

Spencer, R. W. and Braswell, W. D.: How Dry is the Tropical Free Troposphere? Implications for Global Warming Theory, B. Am. Meteor. Soc., 78, 1097–1106, 1997. 3989

Washenfelder, R. A., Toon, G. C., Blavier, J.-F., Yang, Z., Allen, N. T., Wennberg, P. O., Vay, S. A., Matross, D. M., and Daube, B. C.: Carbon dioxide column abundances at the Wis-

AMTD
3, 3987–4007, 2010

consin Tall Tower site, J. Geophys. Res., 111, D22305, doi:10.1029/2006JD007154, 2006. 3988

Worden, J. R., Noone, D., Bowman, K., Beer, R., Eldering, A., Fisher, B., Gunson, M., Goldman, A., Herman, R., Kulawik, S. S., Lampel, M., Osterman, G., Rinsland, C., Rodgers, C., Sander, S., Shephard, M., Webster, C. R., and Worden, H.: Importance of rain evaporation and continental convection in the tropical water cycle, Nature, 445, 528–532, doi:10.1038/nature05508, 2007. 3994

Wunch, D., Toon, G. C., Blavier, J.-F., Washenfelder, R., Notholt, J., Connor, B. J., Griffith, D. W. T., Sherlock, V., and Wennberg, P. O.: The Total Carbon Column Observing Network (TCCON), Philos. T. R. Soc. A, accepted, 2010. 3988

Yang, Z., Toon, G. C., Margolis, J. S., and Wennberg, P. O.: Atmospheric CO_2 retrieved from ground-based near IR solar spectra, Geophys. Res. Lett., 29, 1339, doi:10.1029/2001GL014537, 2002. 3988

AMTD

3, 3987–4007, 2010

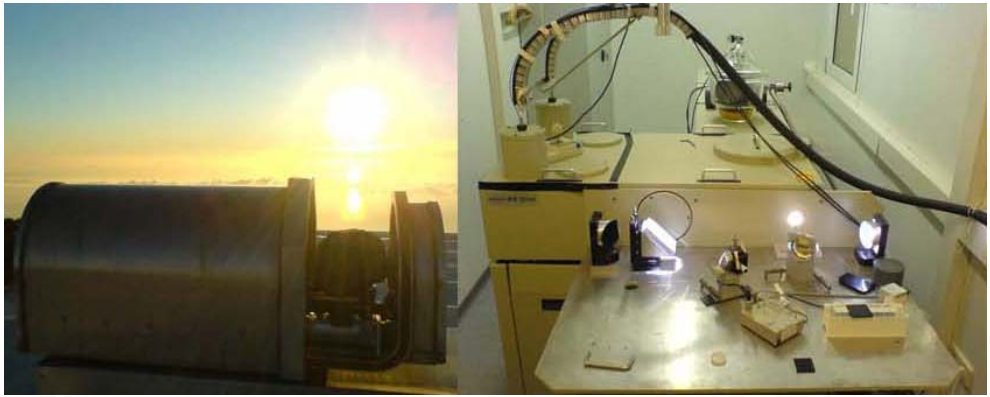

Fig. 1. The TCCON experiment at the Izaña Atmospheric Research Centre. The solar tracker (left photograph) is situated at the top of the experimental housing. It collects the direct solar beam and reflects it into the housing of the FTS (right photograph) where it is coupled into the spectrometer (circular light spot on the right part of the photograph).

AMTD
3, 3987–4007, 2010

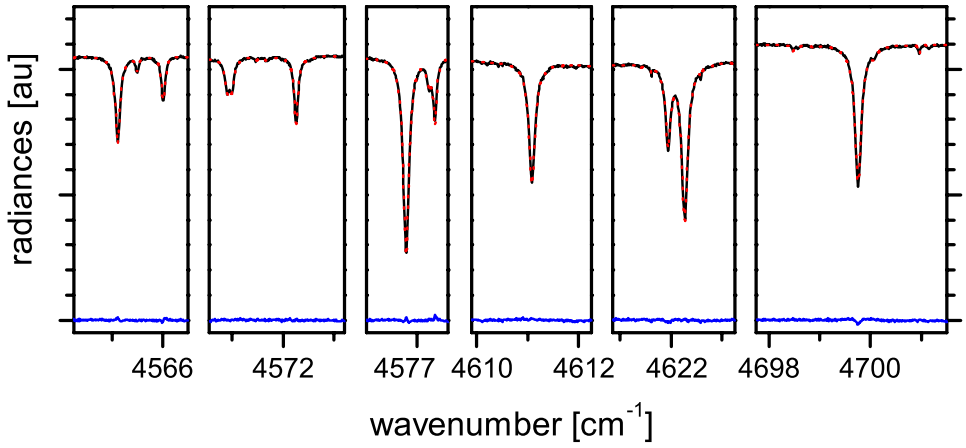

Fig. 2. The used spectral microwindows with H_2O signatures. The shown measurement was taken on the 31st of March 2010, at a solar elevation of 43.4°, and for a total water vapour column amount of 4.7 mm. Black line: measured spectrum; Red line: simulated spectrum; Blue line: residuals (difference between measurement and simulation).

AMTD
3, 3987–4007, 2010

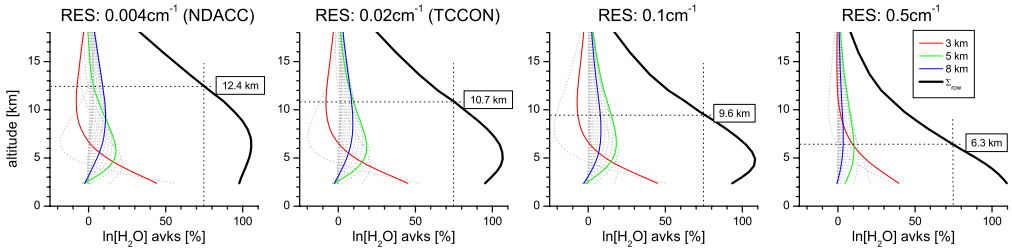

Fig. 3. Averaging kernels for $\ln[H_2O]$ for different spectral resolution. From the left to the right: $0.004\,cm^{-1}$, $0.02\,cm^{-1}$ (resolution of TCCON spectra), $0.1\,cm^{-1}$, and $0.5\,cm^{-1}$. Grey lines: kernels for all atmospheric model grid levels; Black, red, and green lines: kernels for the 3, 5, and 8 km grid level (representative for the lower, middle, and upper troposphere), respectively; Thick black line: Sensitivity (sum along the row of the averaging kernel matrix). Indicated is also the altitude where the sensitivity falls below 75%.

AMTD
3, 3987–4007, 2010

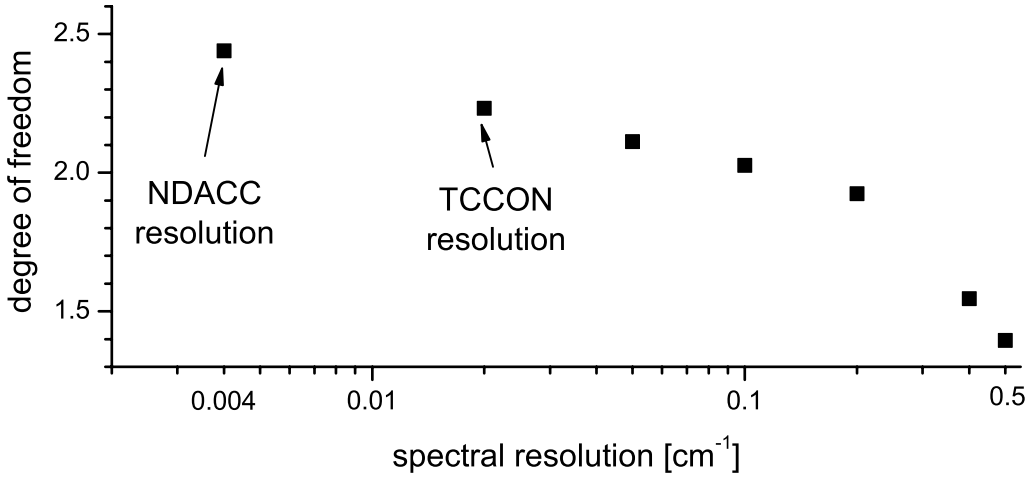

Fig. 4. Degree of freedom of the measurement (dof value) versus spectral resolution.

AMTD
3, 3987–4007, 2010

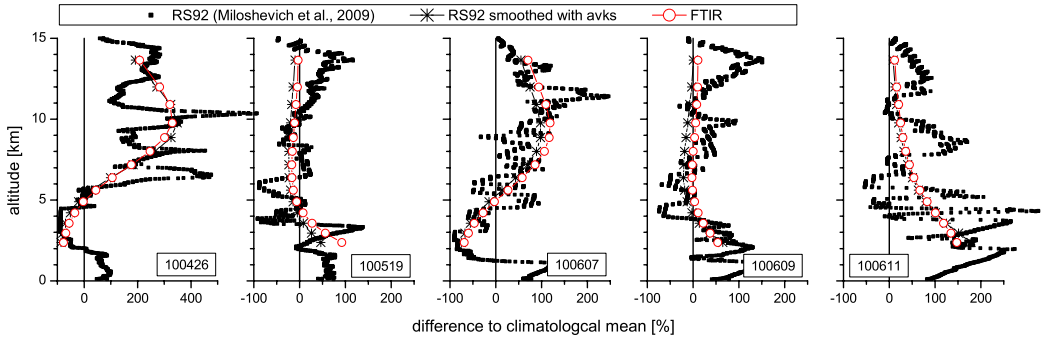

Fig. 5. Comparison of FTIR and Vaisala RS92 H_2O profiles (for April to June 2010 coincidences, i.e., FTIR and RS92 measurements performed within 1 h). Profiles are presented as percentage difference to a subtropical climatological profile. Black squares: RS92 data corrected by the Miloshevich et al. (2009) method; Black stars: RS92 smoothed with FTIR averaging kernels; Red circles: FTIR.

AMTD
3, 3987–4007, 2010

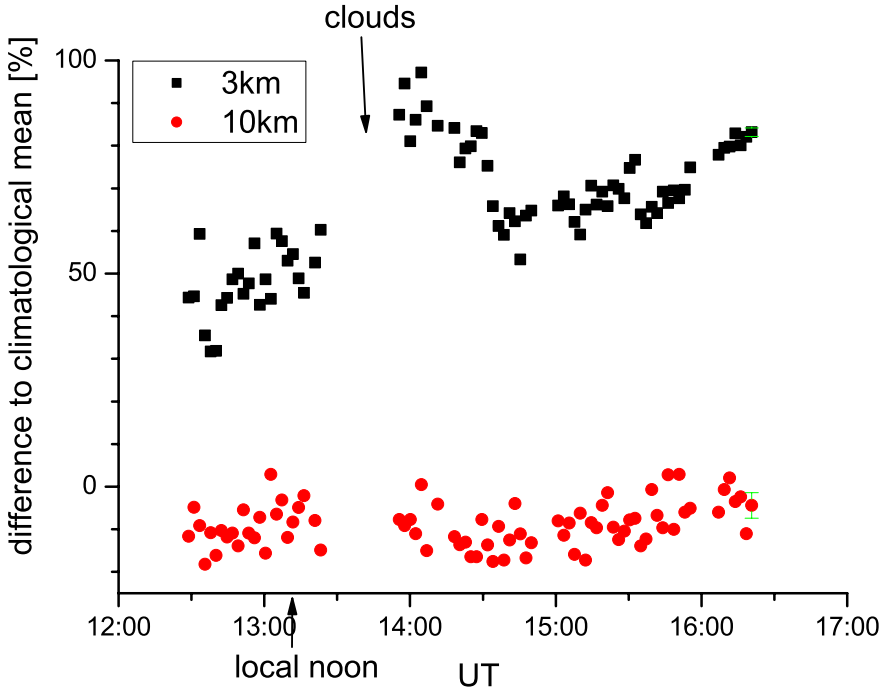

Fig. 6. Evolution of lower (black squares) and upper (red dots) water vapour concentrations between 12:30 and 16:30 UT on the 19th of May 2010. The green error bars indicate the typical uncertainty due to measurement noise.

AMTD
3, 3987–4007, 2010

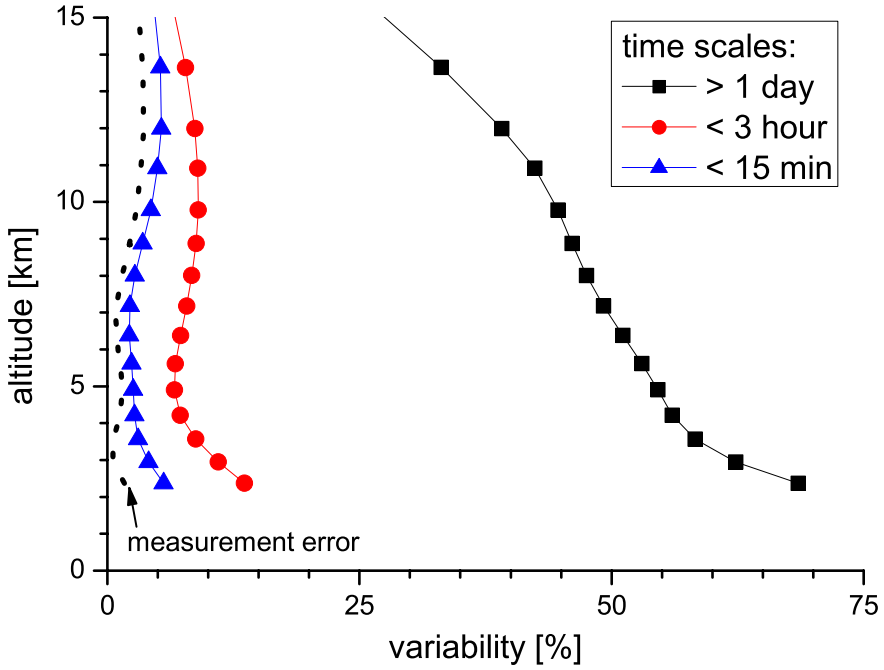

Fig. 7. Profiles of the water vapour variability relative to a mean value for different time scales. Blue: short-time scales (within 1 h); Red: long-time scales (larger than 1 h), Black: overall variability. The dotted black line indicates the typical uncertainty due to measurement noise.

AMTD
3, 3987–4007, 2010